



Journal Name

COMMUNICATION

Tunable Metal-Polyaniline Interface for Efficient Carbon Dioxide Electro-reduction to Formic acid and Methanol in Aqueous Solution

Received 00th January 20xx,
Accepted 00th January 20xx

Weiran Zheng,^{a,b} Simantini Nayak,^a Weizi Yuan,^a Zhiyan Zeng,^c Xinlin Hong,^c Kylie A. Vincent,^a and Shik Chi Edman Tsang^{a,b*}

DOI: 10.1039/x0xx00000x

www.rsc.org/

It is reported that metal on polyaniline (PANI) prepared by a simple method can give excellent electro-reduction activity of CO₂ to HCOOH or CH₃OH due to tunable properties: N atoms on PANI capture CO₂ through a strong Lewis acid-base interaction while Pd atoms, amongst Pd, Pt, Cu, studied, facilitate the fastest proton and electron transfers along PANI to the CO₂ trapped sites to form the best HCOOH yield in highly cooperative manner.

Catalytic conversion of carbon dioxide (CO₂) is considered to be a realistic solution in the reduction of its greenhouse effect. The formation of valuable chemicals or fuels from this route can offset some of the costs for its fixation. Although various conversion methods including thermal catalytic processes are widely explored, the concerns of secondary CO₂ emission prevail, because many of the suggested processes unavoidably involve the input of intense energy in the form of high temperature and pressure, etc. On the other hand, the electrochemical reduction of CO₂ driven by renewable energy sources (wind or solar) appears to be promising. Particularly, the recent dwindling cost of grids from nuclear, hydropower and biomass makes the process even more attractive.¹ However, problems of high over-potential, low current efficiency and poor product selectivity over reported electrocatalysts remain to be solved. The key issue lies in the poor understanding of fundamental chemical and electrochemical steps in the reduction of CO₂ over a selected catalyst on an electrode. If the underlying factors for the multifunctional properties (i.e. CO₂ uptake, H and electron transfers and surface rearrangement) were understood, which could lead a rational design of structure and layout of a composite catalyst for more efficient CO₂ electro-reduction.² Early studies showed that Pb, Zn, Pd, and Cu metal electrodes can produce formic acid from the electro-reduction of CO₂ in

water. Further reduction of the formic acid to hydrocarbons and higher alcohols over metals was also demonstrated.³ However, the use of metal electrodes suffered from the use of high over-potential (almost 1 V) due to weak adsorption of CO₂, and poor product selectivity (a range of C1 to C3 products which included methanol, formic acid, alcohol and propanol together with a large quantity of H₂).^{3b} While the choice of metal catalyst can undoubtedly affect efficiency and selectivity of the products, organic molecules incorporated into the electrode, such as pyridine and N-containing polymers, can play additional role(s) for the electro-reduction.⁴ Nitrogen atoms are known to lower activation energy due to efficient trapping of gaseous CO₂ at the electrode surface.⁵ On the other hand, the use of organic layer(s) as electrodes showed improved current efficiency and product selectivity, but lower intrinsic reaction rates were commonly achieved, presumably due to their poor electronic and H conductivity. Thus, it appears that a composite electrode with metal and N-containing conjugated polymer at the interface could be a useful combination for CO₂ reduction. In addition, size- and shape- controlled metal nanoparticles (NPs) may be synthesized by the use of polymer as stabilizer. However, there have been few studies in using metal/conjugated polymer composite for electrochemical CO₂ reduction in the literature.⁶ For example, a preliminary study of polyaniline(PANI)/Cu₂O composite was reported, which indicated the formation of HCOOH and CH₃COOH in methanol,^{6a} but no work studying the interactions of the catalyst components has yet been initiated.

Here, we report a systematic synthesis of a series of PANI loaded with metal NPs (Pt, Pd, Cu) to establish the composites with extensive metal-PANI interface, which give exceptional activity in the electro-reduction of CO₂ to HCOOH and CH₃OH.

PANI was synthesized using a rapidly mixed reaction in HCl⁷, which was obtained in proton-doped form. The as-synthesized PANI was washed with NH₃·H₂O to remove Cl⁻ (the de-doping process). Notice that PANI contains conjugated benzenoid and quinoid units (Scheme S1) at different ratios to give molecular structures dependent on oxidation states. This ranges from a fully protonated form, the leucoemeraldine (LEB), partially

^a Department of Chemistry, University of Oxford, Oxford, OX1 3QR (UK)

^b Department of Applied Biology and Chemical Technology, Hong Kong Polytechnic University, Hong Kong SAR (P. R. China)

^c College of Chemistry, Wuhan University, Wuhan, 430072 (P. R. China)

* edman.tsang@chem.ox.ac.uk

Electronic Supplementary Information (ESI) available:.

See DOI: 10.1039/x0xx00000x

oxidized emeraldine base (EB) to fully oxidized pernigraniline (PB), as shown in Fig. S1.⁸ For metal/PANI synthesis, PANI (EB form) was dispersed in DMF with metal precursor (metal/N = 1:5). NaBH₄ was added to reduce the metal ions to form metal NPs on PANI at room temperature.

First, our XPS suggested that Cl⁻ was totally removed during the de-doping process (Fig. S1). The SEM image (Fig. S2a) shows that the nanofiber-like morphology with a diameter of 150 nm to 300 nm, indicative of an ordered structure. After *in situ* synthesis of Pd NPs, the metal-PANI composite maintains its shape (Fig. S2b) without changing the PANI structure, as illustrated in Fig. S2c. Similar images were also observed for Cu/PANI and Pt/PANI. The TEM images show that the metal particles are in the nanoscale range with an average diameter ranging from 15.4 nm for Cu NPs (Figure S2d), 2.44 nm for Pd NPs (Figure S2e) to 1.11 nm for Pt NPs (Figure S2f). Their narrow size distributions are given in Fig. S3. Here, the size of metal NPs is much smaller than that of the previous reports due to careful *in situ* synthesis.^{6a,9} It is likely that PANI acts as a stabilizer during the formation of metal NPs. TEM also shows that the metal NPs adopt regular shapes: polyhedral Cu NPs, wormlike Pd NPs and spherical Pt NPs.

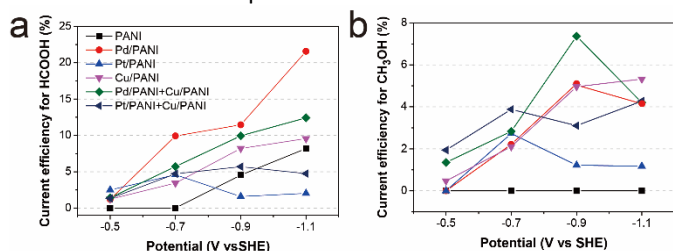


Fig. 1. Current efficiency of (a) HCOOH and (b) CH₃OH over PANI and metal/PANI. Same amount of PANI was used. RDE experiments were run in 0.5 M H₂SO₄ and electrode kept at the target potential for 120 min; the rotating speed was set at 800 rpm.

The CO₂ electrochemical reduction activity in acidic solution of the samples was evaluated on a rotating disk electrode (RDE) in order to minimise mass transfer limitations. The cyclic voltammetry (CV) plot of CO₂ reduction is shown in Fig. S4. Typically, each sample was tested for 2 hours (Pd/PANI as shown in Fig. S5) and then collected for characterization: it showed no structural destruction (Fig. S6). Apart from H₂ and CO₂ in gas phase, only two main liquid products, namely HCOOH and CH₃OH were identified (HCOOH was exclusively formed over the un-promoted PANI) by GC-MS and ¹H-NMR. The current efficiencies of the two products at different potentials, are shown in Fig. 1. According to the figure, the PANI and metal-PANI composites clearly display the ability to produce HCOOH from CO₂ at potentials more negative than -0.5 V vs SHE (Standard hydrogen electrode). Two unique features deserve attention: this system gives significantly lower over-potential and higher selectivity than many reported catalysts⁶ indicative of the impressive nature of the PANI based catalysts for CO₂ reduction (Tables S1, S2). It is apparent that the composites containing metal NPs (in particular Pd) can greatly promote the HCOOH yield at -0.7 V compared to unmodified PANI (Fig. 1a). By applying more negative potentials, a higher yield is obtained for most of the materials, although Pt/PANI shows a decreasing yield from -0.7 V to -1.1

V. This is presumably due to trace CO produced during the reduction of CO₂ that poisons the Pt surface.¹⁰ The highest current efficiency for HCOOH is over 22%, over Pd/PANI at -1.1 V, which shows Pd is the best amongst all the three metals studied. Thus, Pd somehow dramatically promotes the formation of HCOOH rather than the H₂ formation (hydrogen evolution reaction) which is typical of metal catalysts without the polymer support³ (also see ESI) The total CO₂ conversion rate reaches 94.6 mmol/ g·h with 94% selectivity towards HCOOH (Tables S1, S2). As far as we are aware, such current efficiency and particularly the ultra-high selectivity towards HCOOH represent one of the best reported electro-catalytic performances for the CO₂ fixation in this area. Interestingly, as stated, CH₃OH is only formed over the metal (Cu, Pd) /PANI but not at the unmodified PANI (Fig. 1b). Notice that Pd and especially Cu offer active and selective surfaces in thermal catalytic conversion of CO₂/H₂ to CH₃OH.¹¹ This suggests the metal NPs surface in the electrocatalyst is also critical for the formation of methanol. With potential driving force is increased from -0.5 V to -1.1 V, Cu/PANI shows increasing efficiency. Pd/PANI reaches its highest efficiency at -0.9 V, in contrast to Pt/PANI. It is exciting to note that the highest current efficiency for CH₃OH is observed at -0.9 V when the mixture of Pd/PANI and Cu/PANI (molar ratio is 1:1 but keep the same total amount of catalyst) is used. It is apparent from the above study that there are synergetic effects between metal NPs and PANI in the reduction of CO₂ to products, giving methanol productivity of 8.62 mmol/ g·h at 10% current efficiency (Tables S1, S2). We did not get any direct evidence on the formation of alloy (from XRD) during testing the mixture. On the other hand, we cannot exclude the possibility of such formation in small quantity at the materials' interface. Nevertheless, it is envisaged that Pd surface produces [H] at a close proximity to Cu surface which is selective for 'methoxy' adsorption^{11,12} for the final methanol desorption. Work is in progress to shed more light on this mixture. It would be important to elucidate such interactions, which may lead to rational design of new catalysts for efficient CO₂ fixation. Fig. 2a shows the XRD patterns of PANI and metal/PANI. It is well accepted that PANI possesses regular chemical backbones (Scheme S1) hence can be crystallized via H-bonding linkage.¹² The broad peak located at 20.5° (*d* = 4.6 Å) is a characteristic peak of PANI, which is comparable to the literature. Apart from additional diffraction peaks of metals (for Pt/PANI, no metal peak is observed due to the severe peak broadening due to the small Pt NPs size (see Fig. S2f)), it is interesting to note that the peak of PANI in these composites clearly shifts to a larger 2θ value. In the case of Pt/PANI, the peak shifts from 20.5° to 22.0° and in Pd/PANI, further shifts to 22.6°. This implies the highest degree of intermolecular H-bonding packings of PANI units (increasing benzenoid/quinoid ratios) results during the reduction of Pd NPs from the precursor. It is known that a vibrational peak around at 1497 cm⁻¹ assigned to C=C (benzenoid) and a peak at 1588 cm⁻¹ assigned to C=N (quinoid) can be used to assess the redox state of the PANI according to their area ratio (Scheme S1).¹³ FTIR and Raman spectra suggest that the polymer chain remains intact during

metal NPs formation (Figs. S7, S8), showing the same band positions of benzenoid and quinoid structures. After the Pt and Pd metal NPs incorporation, a significant increase in their peak area ratios is evident (Table S3). This once again suggests the extensive reduction of the polymer in the presence of metal NPs. In order to find out how the metal NPs interact with PANI, the XPS region of N_{1s} was analyzed. There are three nitrogen-containing groups within the polymer chain (Fig. 2b): imine ($-N=$ at 398.4 eV), amine ($-NH-$ at 399.6 eV) and small amount of positive charged nitrogen (N^+ at 400.4 eV).¹⁴ With the introduction of Cu NPs, the binding energy (B.E.) of $-N=$ and $-NH-$ remain almost unchanged, while for Pd NPs, the B.E. of $-N=$ clearly shifts to 398.1 eV and $-NH-$ to 399.4 eV (electron promotion from metal to nitrogen). Similarly, there is a small degree of peak shift towards lower B.E. in the Pt NPs indicative of the electron promotion to nitrogen but the easy fouling of Pt surface by contaminants in laboratory (O_2 and CO) despite the careful handling of the samples in inert gas is noted. Nevertheless, the pronounced peak shift in Pd suggests that there is a significant electronic interaction between Pd NPs with the surface nitrogen of PANI nanofibers. But it should be noted that XPS may not be sensitive to reflect the electronic interaction since the majority of nitrogen atoms are not in direct contact with metal NPs (Figs. S2d, S2e and S2f). Characterization of Pd/PANI compared to unmodified PANI by 1H -NMR was also conducted (Fig. S9). The broader shoulder peaks of hydrogen in $-NH-$ group (7.0–7.2 ppm) suggests a wider and increasing population of H atoms in this catalyst during the formation of Pd NPs. Fig. 2c shows the FTIR and CV of PANI and Pd/PANI before and after the treatment with H_2 . There is no change of PANI before or after treatment with H_2 . Interestingly, for Pd/PANI after H_2 treatment, there is a distinctive IR peak shift (C=C stretching vibrations of benzenoid structure) from 1497 to 1509 cm^{-1} . The peak of 1591 cm^{-1} assigned to C=N stretching vibration (quinoid structure) also completely disappears after it is in contact with H_2 . It is well accepted that Pd NPs can dissociate H_2 gas and form surface atomic H even at sub-ambient temperature.¹⁵ But, the complete reduction of PANI by H_2 to form leucoemeraldine (LEB) is still incredible since Pd NPs could not be in touch with all the quinoid units. There implies a long-range efficient H transfer from the metal must occur to lead to extensive reduction of the polymer in remote locations. Fig. 2d shows the CV plots of PANI and Pd/PANI in acidic solution saturated with N_2 and H_2 . Clearly, the protonic benzenoid $-NH$ groups of PANI can be completely oxidized to form quinoid with two oxidation steps between -0.4 V to 0.5 V through its conjugative system: 1. oxidation from the fully reduced form (LEB) to the half-oxidized form (emeraldine salt, ES) at 0 V; 2. oxidation from ES form to fully oxidized form (pernigraniline, PB) at 0.5 V.⁸ Under N_2 , both PANI and Pd/PANI show no hydrogen evolution or oxidation peak in the given range of potentials. However, under H_2 , Pd/PANI shows a sharp peak at -0.04 V, close to the SHE potential. This is a much lower potential for the oxidation of pre-adsorbed H atoms on Pd NPs to protons compared to that of Pd/C of about -0.35 to -0.4 V (Fig. S10). PANI exhibits interesting intra- and intermolecular electronic

and ionic conductivity dependent on oxidation state and pH.¹⁶ This observation is believed to relate to the facilitated H^+ formation from H_2 on Pd surface due to readily electronic flow through conjugation together with high proton flux to PANI via metal-polymer interface during the facile oxidation. Similarly, Pd/PANI and Pt/PANI display higher over-potential for HER than that of Pd/C in N_2 (Fig. S11) due to resilience of proton reduction with reduced PANI of lower electronic conductivity.

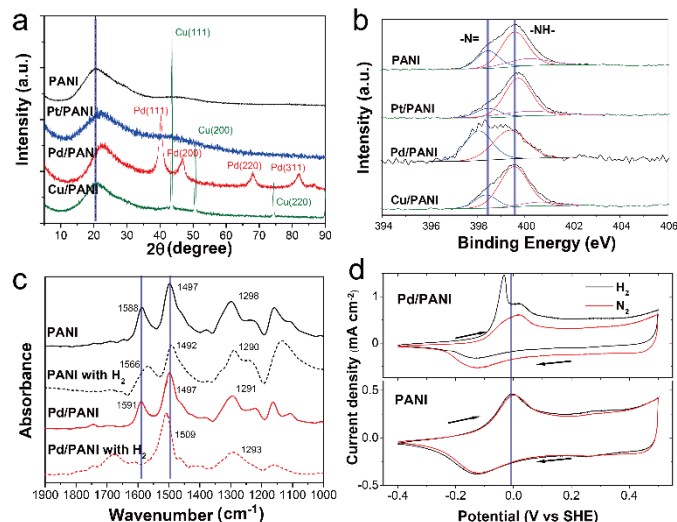


Fig. 2. (a) XRD of PANI, Pt/PANI, Pd/PANI and Cu/PANI; (b) XPS of N_{1s} of PANI, Pt/PANI, Pd/PANI and Cu/PANI; (c) FTIR of PANI and Pd/PANI before and after treatment with H_2 ; (d) CV plots of PANI and Pd/PANI in N_2 and H_2 saturated 0.5 M H_2SO_4 (10th scan shown), scan rate=10 mV/s; rotating speed is 500 rpm.

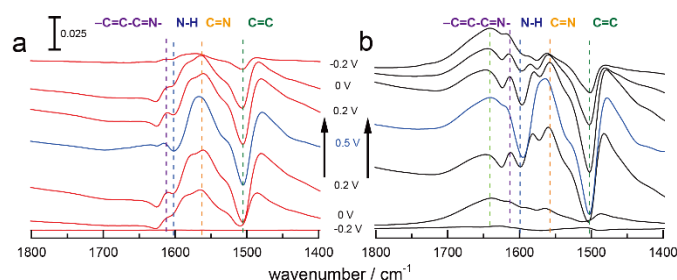


Fig. 3. *In situ* electrochemical ATR-IR of (a) Pd/PANI and (b) PANI under H_2 .

Fig. 3a shows the *in situ* ATR-IR of Pd/PANI and Fig. 3b for PANI at different potentials from -0.3 to 0.5 V at a scan rate of 10 mV/s under H_2 (spectra under N_2 are shown in Fig. S12). All the spectra are processed against a reference recorded at the initial potential, -0.3 V. The peak intensity of C=N peak (PANI: 1558 cm^{-1} , Pd/PANI: 1565 cm^{-1}) increases at the expense of the C=C peak (PANI: 1505 cm^{-1} , Pd/PANI: 1501 cm^{-1}) during oxidation (from -0.2 V to 0.5 V), indicative of increasing quinoid units at the consumption of benzenoid units, and *vice versa* during the reduction. The peak intensity of the N-H deformation (Pd/PANI: 1601 cm^{-1} , PANI: 1595 cm^{-1}) also decreases during the oxidation. The new peak (Pd/PANI: 1611 cm^{-1} , PANI: 1614 cm^{-1}) is considered to be a characteristic vibrational band of PB and can be assigned to a $-C=C=N-$ asymmetrical vibrational mode.¹⁷ Comparing the peak intensity at 0.5 V, PANI is more oxidized than Pd/PANI, suggesting Pd can help to transfer H to PANI for its extensive reduction *via* high electronic and proton conductivity at the

interface (taking up H₂ and forming more N-H structure). Moreover, the PANI suffers change after one cycle (from -0.2 V to 0.5 V to -0.2 V), but it is reversible in the case of Pd/PANI, showing the improved stability with Pd. Thus, Pd metal NPs can exert strong electronic effects with PANI, facilitating electron and H⁺ migration at long range during the redox cycle.

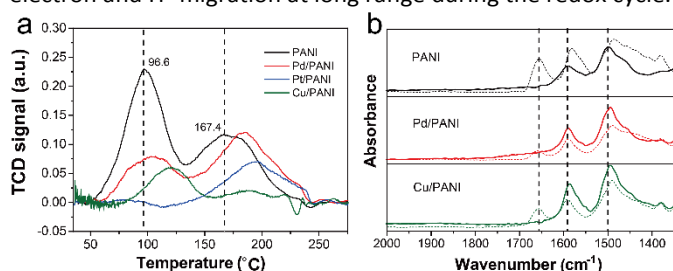
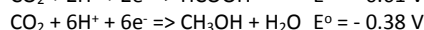
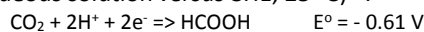


Fig. 4. (a) CO₂ TPD plots of PANI and metal/PANI; (b) FTIR spectra of PANI and metal/PANI before (solid line) and after CO₂ adsorption (dotted line).

The next key questions are: where are the sites for CO₂ capture and why the composites are excellent for CO₂ reduction? Thus, CO₂ adsorptions on PANI and metal/PANI were characterized using CO₂-temperature programmed desorption (TPD) and FTIR (Fig. 4). From the thermogravimetric analysis (TGA), both PANI and metal/PANI are stable until 270 °C (Fig. S14). TPD of PANI depicts two main desorption peaks of 96.6 °C and 167.4 °C, respectively. Pd/PANI also gives the two peaks but at slightly higher temperatures. In cases of Pt/PANI and Cu/PANI, we can only see one dominating signal, 195.0 °C and 125.7 °C, respectively. Thus, PANI can interact with CO₂ mainly in two ways: weak physisorption peak (1st peak) and stronger chemisorption peak (2nd peak). The size of the physisorption peak appears to be related to the surface area of PANI. The strength of CO₂ chemisorption could be reflected by peak temperature (higher electronic density of N atoms promoted by metal gives higher temperature). Clearly, the introduction of metal alters both the adsorption modes. The *in situ* doping on PANI significantly lowers its surface area (aggregation as evidenced by TEM), which decreases the relative physisorption peak size (1st peak, Fig. S15). As to chemisorption of CO₂, Pd and Pt NPs shift the peak to higher temperatures. Significant chemisorption of CO₂ by the metal surface on its own is ruled out since without extensive H, adsorption of CO₂ is not facile.¹⁸ The high over-potential required for electro-chemical reduction of CO₂ over metal electrodes is partly due to its poor adsorption. On the other hand, a significant and comparable quantity of CO₂ can be taken up by PANI and Pd-PANI (Fig. S15). The chemisorbed CO₂ peak (2nd peak size) shifts to higher temperature over Pd/PANI and Pt/PANI as compared to PANI and Cu/PANI. FTIR spectra in Fig. 4b show the appearance of the peak at 1656 cm⁻¹ after CO₂ adsorption, which indicates the formation of stable O-C-O structure. This confirms that CO₂ chemisorption takes place at PANI, Pd/PANI and Cu/PANI (Pt/PANI, similar to Pd/PANI, not shown) through the Lewis acid-base interaction with the polymer N atoms. As a result, the strong CO₂ adsorption by the Lewis basic sites in combination with rapid proton and electron migration from cathode containing noble metal NPs will assist the fast CO₂ hydrogenation to HCOOH. Pd apparently is the best candidate to exert the strong synergetic

effects to conduct H⁺ and electron from water decomposition with PANI to diminish the more favorable H₂ formation via surface H recombination on the metal surface. The fast but long-range reduction of the adsorbed CO₂ of the trapped sites of the PANI polymer will thus give the observed high selectivity towards HCOOH. The slightly higher activation (lower potential of -0.7 V) compared with thermodynamic value of -0.61 V, high selectivity towards HCOOH due to selective trapping and high activity for the fast electron and H⁺ migration in the presence of Pd metal make this system unique. Although Pt shows similar properties as Pd, it is easily fouled during CO₂ to HCOOH. Thermodynamically, CO₂ should be reduced more easily to CH₃OH than HCOOH, as shown below (pH = 7 in aqueous solution *versus* SHE, 25 °C)¹⁹:



However, 'formate' would need to reorganize to 'methoxy' over the metal surface under reduction conditions before methanol can be produced and Cu is well-known to provide such selective surface.¹² As a result, our Pd/PANI provides the best activity for the first stage CO₂ reduction, followed by Cu/PANI for the further reduction of HCOOH to CH₃OH.

In summary, metal/PANI gives high proton and electron migrations between metal NPs and PANI during CO₂ electro-reduction in water with high over-potential for hydrogen evolution. Thus, it can facilitate high activity and selectivity towards HCOOH or CH₃OH without much production of H₂.

Notes and references

- 1 E. E. Benson, C. P. Kubiak, A. J. Sathrum, J. M. Smieja, *Chem. Soc. Rev.* 2009, **38**, 89.
- 2 J. Qiao, Y. Liu, F. Hong, J. Zhang, *Chem. Soc. Rev.* 2014, **43**, 631.
- 3 a)M. Azuma, K. Hashimoto, M. Hiramoto, *J. Electrochem. Soc.* 1990, **137**, 1772. b)K. Kuhl, et al., *JACS.* 2014, **136**, 14107.
- 4 H. Yang, S. Qin, H. Wang, J. X. Lu, *Green Chem.* 2015, **17**, 5144.
- 5 a)L. M. Aeshala, R. Uppaluri, A. Verma, *Phys. Chem. Chem. Phys.* 2014, **16**, 17588. b)A. K. Mishra, S. Ramaprabhu, *J. Mater. Chem.* 2012, **22**, 3708.
- 6 a)A. N. Grace, S. Y. Choi, M. Vinoba, M. Bhagiyalakshmi, D. H. Chu, Y. Yoon, S. C. Nam, S. K. Jeong, *Appl. Energy* 2014, **120**, 85. b)C. Zhao, Z. Yin, J. Wang, *ChemElectroChem* 2015, **2**, 1974. c)K. Ogura, N. Endo, M. Nakayama, *J. Electrochem. Soc.* 1998, **145**, 3801. d)R. Aydin, F. Koleli, *J. Electroanal. Chem.* 2002, **535**, 107.
- 7 J. Huang, R. B. Kaner, *Angew. Chem., Int. Ed.* 2004, **43**, 5817.
- 8 A. G. Macdiarmid et al., *Mol. Cryst. Liq. Cryst.* 1985, **121**, 173.
- 9 B. J. Gallon, R. W. Kojima, R. B. Kaner, P. L. Diaconescu, *Angew. Chem., Int. Ed.* 2007, **46**, 7251.
- 10 S. Akhade, W. Luo, X. Nie, N. J. Bernstein, A. Asthagiri, M. J. Janik, *Phys. Chem. Chem. Phys.* 2014, **16**, 20429.
- 11 L. C. Grabow, M. Mavrikakis, *ACS Catal.* 2011, **1**, 365.
- 12 J. P. Pouget, M. E. Jozefowicz, A. J. Epstein, X. Tang, A. G. MacDiarmid, *Macromolecules* 1991, **24**, 779.
- 13 E. T. Kang, K. G. Neoh, K. L. Tan, *Prog. Polym. Sci.* 1998, **23**, 277.
- 14 S. golczak, A. Kancierzewska, M. Fahlman, K. Langer, J. Langer, *Solid State Ionics* 2008, **179**, 2234.
- 15 K. Nobuhara, H. Kasai, W. A. Diño, H. Nakanishi, *Surf. Sci.* 2004, **566**, 703.
- 16 W. W. Focke, G. E. Wnek, Y. Wei, *J. Phys. Chem.* 1987, **91**, 5813.
- 17 Z. Ping, B. G. E. Nauer, H. Neugebauer, J. Theiner, A. Neckel, *J. Chem. Soc. Faraday Trans.* 1997, **93**, 121.
- 18 A. Bandi, J. Schwarz, C. U. Maier, *J. Electro. Soc.* 1993, **140**, 1006.
- 19 V. P. Indrakanti, J. D. Kubicki, H. H. Schobert, *Energy Environ. Sci.* 2009, **2**, 745.